A Heterojunction Bipolar Transistor Large-signal Model Focused on the Saturation Region

Jongchan Kang, Youngoo Yang, Sungwoo Kim, and Bumman Kim

Department of Electronic and Electrical Engineering and Microwave Application Research Center,
Pohang University of Science and Technology, Pohang, Kyungbuk, 790-784, Korea

Abstract — **We present a new large signal model of HBT for accurately fitting I_C-V_{CE} curve at saturation region with a high level injected collector, which is a very important phenomenon for HBT's. This model treats the saturation as an effective base width modulation and the saturation currents of Ebers-Moll model are modified to include the base width variations. A new empirical function is used to describe the base width modulation. The simulation results using the model follow the measured I_C-V_{CE} curves at the saturation region very well.**

I. INTRODUCTION

Heterojunction bipolar transistors (HBT's) have been widely used for power amplifiers of handsets and a number of papers have been reported to describe accurate large-signal models [1]~[3]. HBT has a heavily doped thin base and rather low-doped thick collector layers. Therefore, the collector layer is in the high level injection at a relatively low current density and the base width is widened. Because of the thin base layer, the base width widening effect of HBT is a lot more severe than that of Si BJT and should be treated properly to get accurate I_C-V_{CE} curves at the saturation region. But so far the strong base widening effect has been neglected for I_C-V_{CE} curve fitting of HBT at the saturation region. Many BJT models [4]~[6] have been upgraded from Kull model [7] to fit the quasi-saturation region concentrating on collector epi-layer phenomenon, such as quasi-saturation, Kirk effect, etc, but still have the problems. This is due to neglecting the base widening effect at the saturation region.

In this paper, we are proposing an improved I_C-V_{CE} curve modeling to solve the problem. Ebers-Moll model is modified to include the base width widening effect. The model is verified by comparing the I_C-V_{CE} characteristics of single-finger and multi-finger HBT's.

II. LARGE SIGNAL MODELLING

We have extracted the model at the saturation from the physical analysis. The modeled device is a single-finger InGaP/GaAs HBT with 2x20um^2 emitter fabricated at POSTECH. The basic epi-structure consists of a 7000Å GaAs collector (3x10^{16}cm^{-3}), a 750Å C-doped GaAs base (4x10^{19}cm^{-3}) and a 400Å InGaP emitter (5x10^{18}m^{-3}). Fig. 1 shows the equivalent circuits including a thermal circuit for self-heating effects and the expressions for the temperature dependent parameters are reproduced from SPICE model [8]. This model is based on Ebers-Moll model [9], [10] and is implemented in Agilent Technologies' advanced design system (ADS) using symbolically defined device (SDD).

A. Bias Independent Parameters

The series resistances of emitter, extrinsic base and collector are extracted from a small-signal model and verified by the physical values calculated from the epi-structure and measured specific contact resistivity by TLM method. The lead inductances of the emitter, base and collector are estimated from the method described by Maas [11], and the pad capacitances are estimated from the method described by Gobert [12]. The estimated values are optimized in the small-signal model and are used in the large signal modeling.

B. Diode Equations and Description of the Base Width Widening

As shown in the Fig. 1, four diodes and one current source are used to describe the E/B and B/C junction currents. I_{BEL} and I_{BCL} are the low-level currents of the emitter-base and collector-base diodes describing the junction leakage, neutral base recombination and surface recombination currents. These diode equations are given by

$$I_{BEL} = I_{SBEL}\exp(\frac{qV_{BE}}{\eta_{BEL}kT} - 1) \tag{1}$$

$$I_{BCL} = I_{SBCL}\exp(\frac{qV_{BC}}{\eta_{BCL}kT} - 1) \tag{2}$$

where I_{SBEL} and I_{SBCL} are the saturation current, η_{BEL} and

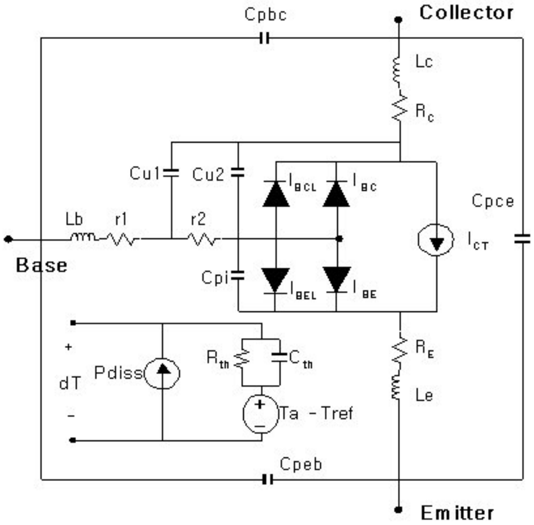

Fig. 1. Equivalent circuits for large-signal model with a thermal circuit for self-heating effect.

η_{BCL} are the ideality factors, and V_{BE} and V_{BC} are the intrinsic junction voltages, respectively. Subscript L indicates the low-current level.

I_{BE}, I_{BC} and I_{CT} describe the normal injection currents and are formulated based on the thermionic emission. These currents are affected by the base width widening at the quasi-saturation region and the effects are included in the saturation current terms as hyperbolic functions. We found that the quasi-saturation itself is not strong enough to describe the I$_C$-V$_{CE}$ curves at the region.

I_{BE} is the base-emitter diode current at a forward bias and is given by,

$$I_{BE} = \frac{I_{SBE}}{\beta_{FT}} \exp(\frac{qV_{BE}}{\eta_{BE}kT} - 1) \tag{3}$$

$$I_{SBE} = \mathrm{K_{SBE}}(\frac{\mathrm{T}}{\mathrm{T_{REF}}})^{(\frac{XTI}{\eta_{BE}}-XTB)} \frac{(\cosh((Wb+wm)/L_B)-1)}{\sinh((Wb+wm)/L_B)} \tag{4}$$

$$\beta_{FT} = \beta_F (\frac{T}{T_{REF}})^{XTB} \tag{5}$$

where Wb is the base layer width, L_B is the electron diffusion length of the base region calculated from the epi-structure and wm is the widened base width. η_{BE} is the ideality factor for the emitter-base forward current and β_{FT} is the forward current gain. To describe the temperature effect on I_{SBE} and β_{FT}, fitting constants of XTI and XTB are used as exponential terms of the ratio for the device temperature T and reference temperature $T_{REF.}$

Similarly to I_{BE}, the collector-base diode current I_{BC} is given by,

$$I_{BC} = \frac{I_{SBC}}{\beta_{RT}} \exp(\frac{qV_{BC}}{\eta_{BC}kT} - 1) \tag{6}$$

$$I_{SBC} = \mathrm{K_{SBC}}(\frac{\mathrm{T}}{\mathrm{T_{REF}}})^{(\frac{XTI}{\eta_{BC}}-XTB)} \frac{(\cosh((Wb+wm)/L_B)-1)}{\sinh((Wb+wm)/L_B)} \tag{7}$$

$$\beta_{RT} = \beta_R (\frac{T}{T_{REF}})^{XTB} \tag{8}$$

where the collector-base saturation current I_{SBC} is also described by hyperbolic functions. Temperature effects are also included in I_{SBC} and reverse current gain β_{RT}. Ideality factor η_{BC} is used for the reverse current.

Collector current source has independent saturation currents and ideality factors and is given by,

$$\begin{aligned} I_{CT} &= I_{CE} + I_{EC} \\ &= I_{SCE}\exp(\frac{qV_{BE}}{\eta_{CE}kT} - 1) + I_{SEC}\exp(\frac{qV_{BC}}{\eta_{EC}kT} - 1) \end{aligned} \tag{9}$$

$$I_{SCE} = K_{SCE} * (\frac{T}{T_{REF}})^{(\frac{XTI}{\eta_{CE}}-XTB)} \frac{1}{\sinh((Wb+wm)/L_B)} \tag{10}$$

where I_{SCE} is also a hyperbolic function of the widened base width wm.

The saturation currents and ideality factors are estimated from the forward and reverse Gummel-plot at reasonable current levels and are optimized from DC simulation assuming that wm equals zero. And then, to fit the quasi-saturation region, wm is included. To describe the base widening effect, we use an empirical function:

$$wm = a_0(1+\tanh(a_1 I_C + a_2))(1-\tanh(a_3 V_{CE} + a_4)) \tag{11}$$

where the widened base width wm is a function of I_C and V_{CE} and a_i are fitting parameters.

The extracted parameters are summarized in Table 1 and Fig. 2 shows the simulation results of I$_C$-V$_{CE}$ curve using the model. The simulated current curve without wm has a large discrepancy from the measured current curve at the quasi-saturation region and this discrepancy is increased as current level increases. The current curve with wm shows a perfect fitting at the quasi-saturation region. Fig. 3 shows wm calculated from the empirical function. As the collector current increases, wm also increases up to 2500Å, which is about 3 times larger than the intrinsic base width. Around V$_{CE}$=1V where the internal collector-base junction goes into reverse bias from forward bias, wm is disappeared. This simulated result shows that the empirical function of wm is sufficiently accurate for the description of the base widening effect. The base widening reduces the current gain at the quasi-saturation region and smoothes out the I$_C$-V$_{CE}$ curves at the knee region. This rounded curve can be described only by the properly modeled *wm*.

param-eter	value	param-eter	value	param-eter	value
Cpeb	37fF	η_{BEL}	1.7	β_R	0.00013
Cpce	17fF	K_{SBC}	4.4e-23	**Wb**	750Å
Cpbc	1.4fF	η_{BC}	1.39	T_{REF}	273K
Lc	96pH	C_{BCL}	1.24	L_B	0.36um
Le	24pH	η_{BCL}	1.68	R_{TH}	1336
Lb	32pH	K_{SCE}	8.6e-21	C_{TH}	10pF
R_E	1.8Ω	η_{CE}	1.38	**a0**	7.08e-6
r1	8Ω	I_{SEC}	7.2e-24	**a1**	134
R_C	7.7Ω	η_{EC}	1.1	**a2**	-5
K_{SBE}	6.3e-18	X_{TI}	0.02	**a3**	2.7
η_{BE}	1.4	X_{TB}	-0.05	**a4**	-0.21
C_{BEL}	0.8	β_F	438		

Table 1. Extracted parameters of single finger HBT(2x20um^2)

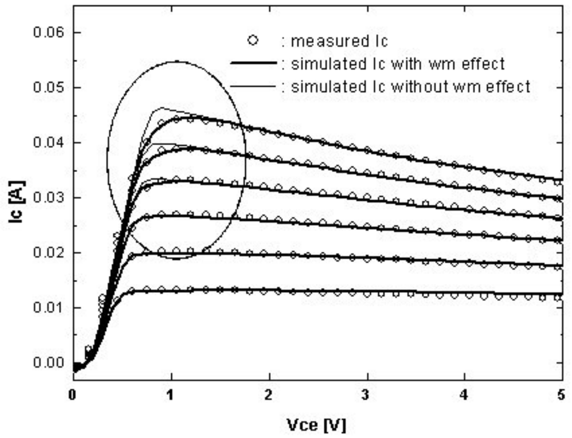

Fig. 2. Measured and simulated I_C-V_{CE} characteristics of single-finger HBT(2x20um^2)

C. Bias dependent Non-linear Parameters

In Fig. 1, *Cpi, Cu1* and *Cu2* represent the bias dependent non-linear parameters of emitter-base capacitance, extrinsic base-collector capacitance and intrinsic base-collector capacitance, respectively. Since this model for a single-finger HBT covers from a low current level to an extremely high current level, the intrinsic base resistance (*r2*) is treated as a base current dependent parameter following the distributed nature of the base current. These non-linear parameters are extracted from the large signal model fitting to the measured S-parameters at the multi-bias points and then represented by empirical functions dependent on currents and junction voltages.

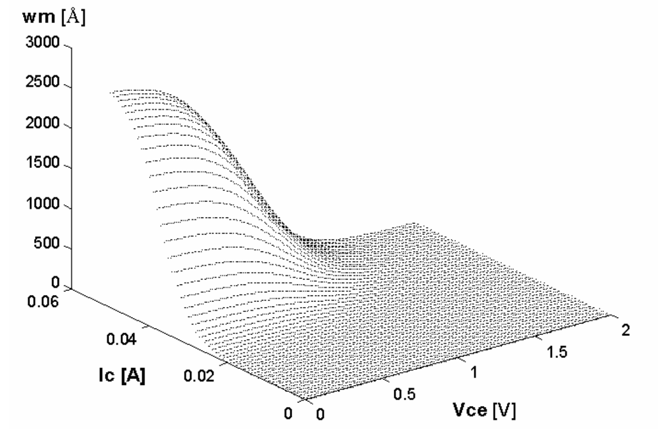

Fig. 3. Simulation result of modulated base width from the empirical function

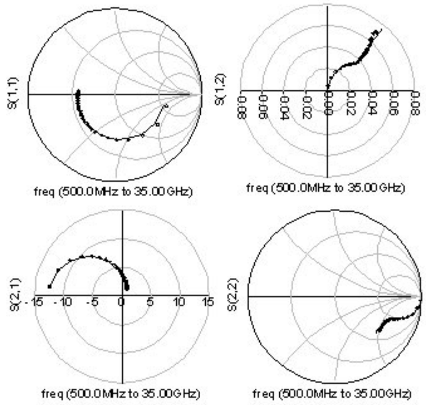

Fig. 4. Measured and simulated S-parameters of single-finger HBT(2x20um^2) at Vce=3.5V, Ic=25mA

To verify the non-linear parameter functions, measured S-parameters throughout the frequency range from 0.5 to 35 GHz are compared with simulated ones. Fig. 4 shows the comparisons of the S-parameters at V_{CE}=3.5V, IC=25mA with good agreements.

D. Model Application to the Multi-finger HBT

This model is applied to a multi-finger HBT. Since epi-structure is not known, emitter and collector resistances are estimated from Z-parameters converted from the measured small signal S-parameters [11] and the extrinsic base resistance is estimated from the method described by Gobert [12]. Base width and doping concentration are assumed as 1000Å and 4x10^{19}, respectively. Other parameters are determined by the same way as the single-finger HBT.

param-eter	value	param-eter	value	param-eter	value
Cpeb	0.44pF	η_{BEL}	1.71	β_R	0.001
Cpce	0.3pF	K_{SBC}	9.9e-22	**Wb**	1000Å
Cpbc	0.12pF	η_{BC}	1.24	T_{REF}	273K
Lc	65pH	C_{BCL}	15	L_B	0.36um
Le	8.6pH	η_{BCL}	1.5	R_{TH}	817
Lb	14.3pH	K_{SCE}	4.6e-20	C_{TH}	10pF
R_E	0.7Ω	η_{CE}	1.32	**a0**	1.8e-5
r1	1.56Ω	I_{SEC}	2.1e-21	**a1**	15
R_C	0.98Ω	η_{EC}	1.05	**a2**	-3
K_{SBE}	4.9e-16	X_{TI}	1.35	**a3**	4.5
η_{BE}	1.44	X_{TB}	-0.0002	**a4**	-1.82
C_{BEL}	0.4	β_F	386		

Table 2. Extracted parameters of multi-finger HBT

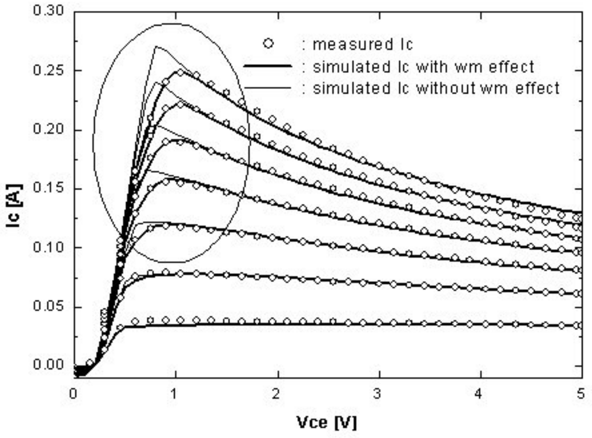

Fig. 5. Measured and simulated I_C-V_{CE} characteristics of multi-finger HBT

Table 2 shows the extracted parameters and Fig. 5 shows the measured and simulated results of I_C-V_{CE} curves of the multi-finger HBT. The comparison results are similar to those of the single-finger HBT.

III. CONCLUSION

A large signal model focused on the quasi-saturation region is presented. This model incorporates the saturation effect as a base widening and this effective base width is included in the modified Ebers-Moll model as a hyperbolic function. Agilent Technologies' ADS is used to implement this model using the symbolically defined device (SDD). From the comparison of the measured and simulated I_C-V_{CE} results, this model is proved to describe the saturation region accurately.

REFERENCES

[1] P. C. Grossman and J. Choma, "Large-signal modeling of HBT's including self-heating and transit time effects," *IEEE Trans. Microwave Theory Tech*. vol. 40, p. 35, Jan 1993.

[2] J. J. Liou, L. L, C. I. Huang and B. Bayraktaroglu, "A Physics Based, Analytical Heterojunction Bipolar Transistor Model Including Thermal and High-Current Effects," *IEEE Trans. Electron devices.*, vol. 40, p. 1570, Sep. 1993.

[3] Q. M. Zhang, H. Hu, J. Sitch, R. K. Surridge and J. M. Xu, "A New large Signal HBT Model," *IEEE Trans. Microwave Theory Tech.*, vol. 44, No. 11, Nov. 1996.

[4] H. C. de Graff and W. J. Kloosterman, "Modeling of the collector epi-layer of a bipolar transistor in the Mextram model," *IEEE Trans. Electron Devices*, vol. 42, p. 274, Feb. 1995.

[5] J. C. J. Paasschens, W. J. Kloosterman, R. J. Havens and H. C. de Graff "Improved Compact Modeling of Output Conductance and Cutoff Frequency of Bipolar Tranistors," *IEEE J. of Solid-State Circuits*, vol. 36, No. 9, September 2001.

[6] C. C. McAndrew, J. A. Seitchik, D. F. Bowers, M. Dunn, M. Foisy, I. Getreu, M. Mc Swain, S. Moinian, J. Parker, D. J. Roulston, M. Schröter, P. van Wijnen and L. F. Wagner, "Vbic95 the vertical bipolar inter-company model," *IEEE J. of Solid-State Circuits*, vol. 31, p. 1476, Oct. 1996.

[7] G. M. Kull, L. W. Nagel, S. W. Lee, P. Lloyd, E. J. Prendergest and H. Dirks, "A unified circuit model for bipolar transistors including quasi-saturation effects," *IEEE Trans. Electron devices.*, vol. ED-32, p. 1103, June 1985.

[8] G. Massobrio and P. Antognetti, "*Semiconductor Device Modeling with SPICE*" Mcgrow Hill, 2nd Edition, 1993.

[9] E. Getreu, "*Modeling the Bipolar Transistor*" Beaverton: Tektronics Inc, 1976.

[10] R. F. Pierret, "*Semiconductor Device Fundamentals*" Addison-Wesley, pp. 389~407 1996.

[11] S. A. Mass and D. Tait, "Parameter-extraction method for heterojunction bipolar transistors," *IEEE Microwave Guided wave Lett.,* vol. 2, December 1992.

[12] Y. Gobert, P. J. Tasker and K. H. Bachen, "A physical, Yet Simple, Small-Signal equivalent Circuit for the Heterojunction Bipolar Transistors," *IEEE Trans. Microwave Theory Tech.*, vol. 45, January 1997.